



HAL
open science

Gamma irradiation-induced absorption in single-domain and periodically-poled KTiOPO₄ and Rb:KTiOPO₄

R.S. Coetzee, S. Duzellier, J.B. Dherbecourt, A. Zukauskas, M. Raybaut, V. Pasiskevicius

► **To cite this version:**

R.S. Coetzee, S. Duzellier, J.B. Dherbecourt, A. Zukauskas, M. Raybaut, et al.. Gamma irradiation-induced absorption in single-domain and periodically-poled KTiOPO₄ and Rb:KTiOPO₄. *Optical Materials Express*, 2017, 7 (11), p. 4138-4146. 10.1364/OME.7.004138 . hal-01632663

HAL Id: hal-01632663

<https://hal.science/hal-01632663>

Submitted on 10 Nov 2017

HAL is a multi-disciplinary open access archive for the deposit and dissemination of scientific research documents, whether they are published or not. The documents may come from teaching and research institutions in France or abroad, or from public or private research centers.

L'archive ouverte pluridisciplinaire **HAL**, est destinée au dépôt et à la diffusion de documents scientifiques de niveau recherche, publiés ou non, émanant des établissements d'enseignement et de recherche français ou étrangers, des laboratoires publics ou privés.



Gamma irradiation-induced absorption in single-domain and periodically-poled KTiOPO_4 and Rb:KTiOPO_4

R. S. COETZEE,^{1,*} S. DUZELLIER,² J. B. DHERBECOURT,² A. ZUKAUSKAS,¹
M. RAYBAUT,² AND V. PASISKEVICIUS¹

¹*Department of Applied Physics, Royal Institute of Technology, Roslagstullsbacken 21, 10691 Stockholm, Sweden*

²*ONERA, The French Aerospace Lab, Chemin de la Hunière, 91761 Palaiseau, France*

**rc@laserphysics.kth.se*

Abstract: We investigate the effect of gamma radiation on flux grown KTiOPO_4 and Rb:KTiOPO_4 samples, as well as their periodically poled variants. Specifically, we study the altered transmission due to color-center formation via gamma irradiation. We measured the transmission of our samples for varying radiation doses and demonstrate effective temperature annealing of gamma radiation induced color centers. We measured a maximum transmission difference of 2% in our samples, which was easily corrected with temperature annealing. No long term and permanent changes were found to be induced in our samples.

© 2017 Optical Society of America under the terms of the [OSA Open Access Publishing Agreement](#)

OCIS codes: (140.3330) Laser damage; (190.4400) Nonlinear optics, materials.

References and links

1. ASCENDS Workshop Steering Committee, Active Sensing of CO_2 Emissions over Nights, Days, and Seasons (ASCENDS) Mission NASA Science Definition and Planning Workshop Report (2008).
2. P. Ciais, D. Crisp, H. Denier van der Gon, R. Engelen, G. Janssens-Maenhout, M. Heiman, P. Rayner, and M. Scholze, Towards a European Operational Observing System to Monitor Fossil CO_2 Emissions, Final Report from the expert group, European Commission (2015).
3. D. K. Killinger and N. Menyuk, "Remote probing of the Atmosphere using a CO_2 DIAL system," *IEEE J. Quantum Electron.* **17**, 1917–1929 (1981).
4. M. Raybaut, T. Schmid, A. Godard, A. K. Mohamed, M. Lefebvre, F. Marnas, P. Flamant, A. Bohman, P. Geiser, and P. Kaspersen, "High-energy single-longitudinal mode nearly diffraction-limited optical parametric source with 3 MHz frequency stability for CO_2 DIAL," *Opt. Lett.* **34**(13), 2069–2071 (2009).
5. A. Amediek, A. Fix, M. Wirth, and G. Ehret, "Development of an OPO system at 1.57 μm for integrated path DIAL measurement of atmospheric carbon dioxide," *Appl. Phys. B* **92**, 295–302 (2008).
6. A. Eldering, C. W. O'Dell, P. O. Wennberg, D. Crisp, M. R. Gunson, C. Viatte, C. Avis, A. Braverman, R. Castano, A. Chang, L. Chapsky, C. Cheng, B. Connor, L. Dang, G. Doran, B. Fisher, C. Frankenberg, D. Fu, R. Granat, J. Hobbs, R. A. M. Lee, L. Mandrake, J. McDuffie, C. E. Miller, V. Myers, V. Natraj, D. O'Brien, G. B. Osterman, F. Oyafuso, V. H. Payne, H. R. Pollock, I. Polonsky, C. M. Roehl, R. Rosenberg, F. Schwandner, M. Smyth, V. Tang, T. E. Taylor, C. To, D. Wunch, and J. Yoshimizu, "The Orbiting Carbon Observatory-2: First 18 months of science data products," *Atmos. Meas. Tech.* **10**, 549–563 (2017).
7. D. M. Hammerling, A. M. Michalak, C. O'Dell, and S. R. Kawa, "Global CO_2 distributions over land from the Greenhouse Gases Observing Satellite (GOSAT)," *Geophys. Res. Lett.* **39**, L08804 (2012).
8. Y. Durand, J. Caron, P. Bensi, P. Ingmann, J.-L. Bézy, and R. Meynard, "A-SCOPE: concepts for an ESA mission to measure CO_2 from space with a lidar," in *8th International Symposium on Tropospheric Profiling*, A. Apituley, H. W. J. Russchenberg, and W. A. A. Monna, eds. (2008), pp. 37–40.
9. Q. Wang, J. Geng, and S. Jiang, "2- μm Fiber Laser Sources for Sensing," *Opt. Eng.* **53**, 61609 (2014).
10. U. N. Singh, B. M. Walsh, J. Yu, M. Petros, M. J. Kavaya, T. F. Refaat, and N. P. Barnes, "Twenty years of Tm:Ho:YLF and LuLiF laser development for global wind and carbon dioxide active remote sensing," *Opt. Mater. Express* **5**(4), 827 (2015).
11. D. J. Armstrong, W. J. Alford, T. D. Raymond, A. V. Smith, and M. S. Bowers, "Parametric amplification and oscillation with walkoff-compensating crystals," *J. Opt. Soc. Am. B* **14**, 460 (1997).
12. G. Arisholm, E. Lippert, G. Rustad, and K. Stenersen, "Efficient conversion from 1 to 2 microm by a KTP-based ring optical parametric oscillator," *Opt. Lett.* **27**(15), 1336–1338 (2002).
13. D. J. Armstrong and A. V. Smith, "All solid-state high-efficiency tunable UV source for airborne or satellite-based ozone DIAL systems," *IEEE J. Sel. Top. Quantum Electron.* **13**, 721–731 (2007).
14. G. Stoeppler, N. Thilmann, V. Pasiskevicius, A. Zukauskas, C. Canalias, and M. Eichhorn, "Tunable Mid-

- infrared ZnGeP₂ RISTRA OPO pumped by periodically-poled Rb:KTP optical parametric master-oscillator power amplifier,” *Opt. Express* **20**(4), 4509–4517 (2012).
15. B. Jacobsson, V. Pasiskevicius, F. Laurell, E. Rotari, V. Smirnov, and L. Glebov, “Tunable narrowband optical parametric oscillator using a transversely chirped Bragg grating,” *Opt. Lett.* **34**(4), 449–451 (2009).
 16. M. Henriksson, M. Tiihonen, V. Pasiskevicius, and F. Laurell, “ZnGeP₂ parametric oscillator pumped by a linewidth-narrowed parametric 2 microm source,” *Opt. Lett.* **31**(12), 1878–1880 (2006).
 17. A. Zukauskas, N. Thilmann, V. Pasiskevicius, F. Laurell, and C. Canalias, “5 mm thick periodically poled Rb-doped KTP for high energy optical parametric frequency conversion,” *Opt. Mater. Express* **1**, 201 (2011).
 18. B. Boulanger, F. Laurell, C. Canalias, V. Pasiskevicius, and A. Pen, “Bulk PPKTP by crystal growth from high temperature solution,” *J. Cryst. Growth* **360**, 52 (2011).
 19. F. Bach, M. Mero, V. Pasiskevicius, A. Zukauskas, and V. Petrov, “High repetition rate, femtosecond and picosecond laser induced damage thresholds of Rb:KTiOPO₄ at 1.03 μm,” *Opt. Mater. Express* **7**, 744–750 (2015).
 20. R. S. Coetzee, N. Thilmann, A. Zukauskas, C. Canalias, and V. Pasiskevicius, “Investigations of laser induced damage in KTiOPO₄ and Rb:KTiOPO₄ at 1 μm and 2 μm,” *Opt. Mater. Express* **5**, 2090–2095 (2015).
 21. A. Hildenbrand, F. R. Wagner, J.-Y. Natoli, M. Commandre, H. Albrecht, and F. Théodore, “Laser damage investigation in nonlinear crystals: Study of KTiOPO₄ (KTP) and RbTiOPO₄ (RTP) crystals,” *Proc. SPIE* **6998**, 699815 (2008).
 22. F. R. Wagner, G. Duchateau, J. Y. Natoli, H. Akhouayri, and M. Commandré, “Catastrophic nanosecond laser induced damage in the bulk of potassium titanyl phosphate crystals,” *J. Appl. Phys.* **115**, 243102 (2014).
 23. M. P. Scricsick, D. N. Lolocono, J. Rottenberg, S. H. Goellner, L. E. Halliburton, and F. K. Hopkins, “Defects responsible for gray tracks in flux-grown KTiOPO₄,” *Appl. Phys. Lett.* **66**, 3428–3430 (1995).
 24. B. Boulanger, I. Rousseau, J. P. Fève, M. Maglione, B. Ménaert, and G. Marnier, “Optical Studies of Laser-Induced Gray-Tracking in KTP,” *IEEE J. Quantum Electron.* **35**, 281–286 (1999).
 25. S. Wang, V. Pasiskevicius, and F. Laurell, “Dynamics of green light-induced infrared absorption in KTiOPO₄ and periodically poled KTiOPO₄,” *J. Appl. Phys.* **96**, 2023 (2004).
 26. J. Hirohashi, V. Pasiskevicius, S. Wang, and F. Laurell, “Picosecond blue-light-induced infrared absorption in single-domain and periodically poled ferroelectrics,” *J. Appl. Phys.* **101**, 33105 (2007).
 27. S. Tjörnhammar, V. Maestroni, A. Zukauskas, T. K. Uždavinys, C. Canalias, F. Laurell, and V. Pasiskevicius, “Infrared absorption in KTP isomorphs induced with blue picosecond pulses,” *Opt. Mater. Express* **5**, 2951 (2015).
 28. M. G. Roelofs, “Identification of Ti³⁺ in potassium titanyl phosphate and its possible role in laser damage,” *J. Appl. Phys.* **65**, 4976–4982 (1989).
 29. G. J. Edwards, M. P. Scricsick, L. E. Halliburton, and R. F. Belt, “Identification of a radiation-induced hole center in KTiOPO₄,” *Phys. Rev. B* **48**, 6884–6891 (1993).
 30. A. Zukauskas, V. Pasiskevicius, and C. Canalias, “Second-harmonic generation in periodically poled bulk Rb-doped KTiOPO₄ below 400 nm at high peak-intensities,” *Opt. Express* **21**(2), 1395–1403 (2013).
 31. M. J. Harris, “Spatial and temporal variability of the gamma radiation from Earth’s atmosphere during a solar cycle,” *J. Geophys. Res.* **108**, 1435 (2003).
 32. A. Ciapponi, W. Riede, G. Tzeremes, H. Schröder, and P. Mahnke, “Non-linear optical frequency conversion crystals for space applications,” *Proc. SPIE* **7912**, 791205 (2011).
 33. U. Roth, M. Tröbs, T. Graf, J. E. Balmer, and H. P. Weber, “Proton and gamma radiation tests on nonlinear crystals,” *Appl. Opt.* **41**(3), 464–469 (2002).
 34. M. V. Alampiev, O. F. Butyagin, and N. I. Pavlova, “Optical absorption of gamma-irradiated KTP crystals in the 0.9 — 2.5 μm range,” *Quantum Electron.* **30**, 255–256 (2000).
 35. B. R. Bhat, N. Upadhyaya, and R. Kulkarni, “Total radiation dose at geostationary orbit,” *IEEE Trans. Nucl. Sci.* **52**, 530–534 (2005).
 36. K. P. Ray, E. G. Mullen, T. E. Bradley, D. M. Zimmerman, and E. A. Duff, “A comparison between ⁶⁰Co ground tests and CRRES space flight data,” *IEEE Trans. Nucl. Sci.* **39**, 1851–1858 (1992).
 37. H. Prieto-Alfonso, L. Del Peral, M. Casolino, K. Tsuno, T. Ebisuzaki, and M. D. Rodríguez Frias, “Radiation hardness assurance for the JEM-EUSO space mission,” *Reliab. Eng. Syst. Saf.* **133**, 137–145 (2015).
 38. G. J. Brucker, E. G. Stassinopoulos, O. Van Gunten, L. S. August, and T. M. Jordan, “The damage equivalence of electrons, protons, and gamma rays in MOS devices,” *IEEE Trans. Nucl. Sci.* **29**, 1966–1969 (1982).
 39. “Total dose steady-state irradiation test method,” ESA, ESCC, Basic Specif. No. **22900**, 1–17 (2010).
 40. G. Hansson, H. Karlsson, S. Wang, and F. Laurell, “Transmission measurements in KTP and isomorphous compounds,” *Appl. Opt.* **39**(27), 5058–5069 (2000).
 41. M. J. Berger, J. H. Hubbell, S. M. Seltzer, J. Chang, J. S. Coursey, R. Sukumar, D. S. Zucker, and K. Olsen, *XCOM: Photon Cross Section Database (Version 1.5)*. (National Institute of Standards and Technology, Gaithersburg, MD, 2010).
 42. P. V. Murphy and B. Gross, “Polarization of Dielectrics by Nuclear Radiation. II. Gamma-Ray-Induced Polarization,” *J. Appl. Phys.* **35**, 171–174 (1964).
 43. G. Wilson, J. R. Dennison, A. E. Jensen, and J. Dekany, “Electron energy-dependent charging effects of multilayered dielectric materials,” *IEEE Trans. Plasma Sci.* **41**, 3536–3544 (2013).
 44. Q. Jiang, M. N. Womersley, P. A. Thomas, J. P. Rourke, K. B. Hutton, and R. C. C. Ward, “Ferroelectric, conductive, and dielectric properties of KTiOPO₄ at low temperature,” *Phys. Rev. B* **66**, 94102 (2002).

45. G. Rosenman, A. Skliar, I. Lareah, N. Angert, M. Tseitlin, and M. Roth, "Observation of ferroelectric domain structures by secondary-electron microscopy in as-grown KTiOPO_4 crystals," *Phys. Rev. B Condens. Matter* **54**(9), 6222–6226 (1996).
46. W. Y. Ching and Y.-N. Xu, "Band structure and linear optical properties of KTiOPO_4 ," *Phys. Rev. B Condens. Matter* **44**(10), 5332–5335 (1991).
47. K. T. Stevens, N. C. Giles, and L. E. Halliburton, "Photoluminescence and micro-Raman studies of as-grown and high-temperature-annealed KTiOPO_4 ," *Appl. Phys. Lett.* **68**, 897 (1995).
48. M. J. Martín, D. Bravo, R. Solé, F. Díaz, F. J. López, and C. Zaldo, "Thermal reduction of KTiOPO_4 single crystals," *J. Appl. Phys.* **76**, 7510–7518 (1994).

1. Introduction

Further improvement of climate models and better understanding of the shifting radiative power balance in the Earth's atmosphere requires increasingly accurate measurements of greenhouse gases (CO_2 , CH_4 , etc.) concentration distribution in the atmosphere on the global scale [1,2]. Ground-based and airborne LIDAR schemes, based on differential absorption lidar (DIAL), are currently employed to achieve the required sensitivity [2–5]. Determining the global concentration distributions and their dynamics however requires spaceborne LIDAR instruments to improve on the data produced by the passive spaceborne instruments [1,2,6,7]. For this reason several DIAL LIDAR missions have been proposed and are under active development [1,8]. Targeting the 2 μm spectral region is beneficial due to the possibility to simultaneously access several gas species, including CO_2 , CH_4 and H_2O . A spaceborne DIAL LIDAR instrument typically requires substantial pulse energy of tens of mJ delivered in transform-limited nanosecond pulses with rapidly tunable central wavelength. Although solid state and fiber lasers based on Tm^{3+} , Ho^{3+} are being investigated for LIDAR applications [9,10], the coherent light sources based on optical parametric oscillators and amplifiers remain the most viable technology for the active spaceborne multispecies gas sensing instruments today. Pulsed parametric sources based on optical parametric oscillators (OPO's) and optical parametric amplifiers (OPA's) are well suited for such applications, due to their high-energy output, high overall efficiencies, broad tunability and access to wavelengths within the mid-infrared.

For such schemes operating around 2 μm and pumped with well-established 1 μm lasers, type-II phase matched KTiOPO_4 (KTP) is widely used as the gain material owing to its high-damage threshold, narrow gain bandwidth, relatively high nonlinearity and broad transparency. Owing to the critical phase matching, multi-crystal walk-off compensating arrangements [4,11,12] or more elaborate OPO cavities with image-rotation [13,14] are usually employed to increase the output beam quality. Tuning in such arrangements involves precise rotation of pair of crystals in opposite direction and represents an additional and unwelcome complication in the LIDAR systems which need to operate unattended.

Due to the ferroelectric nature of KTP, it may be periodically poled, thereby employing quasi-phase matching (QPM) to yield substantially higher effective nonlinearity and noncritical phase matching. At the same time, the large parametric gain bandwidth obtained close to degeneracy obviates the need for angular tuning arrangements in OPA's and OPO's [14–16]. Recently we demonstrated that homogeneous large-aperture QPM structures can be fabricated in Rb:KTP, suitable for high-energy mid-infrared generation [17]. Periodically poled KTP (PPKTP) and Rb:KTP (PPRKTTP) show similar or higher laser induced catastrophic damage threshold as single-domain KTP and Rb:KTP [18–22]. The catastrophic optical damage can be readily avoided by judiciously choosing optical intensities in the system design. The high effective nonlinearity in PPKTP and PPRKTTP provides for large design margins. For long-term unattended system operation within a space environment it is important to consider other effects which could degrade the system performance.

All nonlinear crystals, to a different degree, are susceptible to formation of infrared-absorbing color centers produced by exposure to parasitic blue-ultraviolet optical radiation and ionizing radiation in space environment. Blue and green -light induced infrared absorption have been studied before in KTP, Rb:KTP as well as PPKTP and PPRKTTP [23–

27]. The color centers which are responsible for near-infrared absorption in KTP isomorphs are related to polarons formed by self-trapped photo-generated electrons and holes in proximity to Ti^{4+} and O^{2-} ions, respectively [27–29]. It was shown that Rb-doping of KTP with concentrations of about 1% strongly reduces accumulation of the induced color centers, making PPRKTP superior in terms of quality of the large-aperture QPM structures and in terms of performance at high-average and peak-powers [30]. In contrast to catastrophic laser-induced damage, it is well known that the color centers in KTP isomorphs can be removed by annealing at temperatures above $\sim 100^\circ\text{C}$.

For spaceborne LIDAR systems, the nonlinear crystals are not only subject to laser radiation, but also to the ionizing radiation from energetic electrons, protons and heavier ions originating from the Sun and cosmic rays, as well as gamma rays produced by collisions of the energetic particles with ions in the upper layers of the Earth atmosphere [31]. The radiation can create free carriers and introduce new defects in the nonlinear materials which, in turn give rise to additional linear absorption and leads to degradation of the device performance. The influence of gamma and proton radiation on transmission properties in commercially tradeable KTP and other nonlinear crystals has been previously studied with the focus on second-harmonic generation at 532 nm [32,33]. It was found that the SHG efficiency decreased by about 15% after exposure to 139 krad dose of gamma radiation, primarily caused by the decrease in the linear transmission in the spectral range around 500 nm. On the other hand the transmission of KTP at 1 μm was only weakly modified by doses as high as 1000 krad [34]. Susceptibility of the periodically poled KTP and Rb:KTP has not been investigated so far. Assuming that some of the induced absorption is owing to the color-centers of similar nature as produced by the UV radiation we might expect that it would be possible to devise a procedure for thermal annealing whereby the effects of the ionizing radiation are mitigated. In this work we investigate the effects of different doses of gamma radiation on the linear transmission properties in single domain KTP, a weakly doped Rb:KTP ($[\text{Rb}]/[\text{K}] < 0.01$) as well as PPKTP and PPRKTP QPM structures designed for operation in 2 μm LIDAR. The measurements cover the entire transmission range of the crystals. Our results show that the main increase in absorption is contained in the visible spectral range and is somewhat weaker in the QPM structures. Furthermore, we show that thermal annealing at 150°C is effective in removing the induced color centers.

2. Experimental procedures

Before discussing the experimental procedures it is important to estimate the cumulative dose and the dose rate that the LIDAR instrument could be exposed to on board a satellite. Most of the protons and electrons are trapped by the Earth's magnetic field within van Allen radiation belts, so the total expected radiation dose during the mission strongly depends on the actual orbit of the satellite, shielding, as well as the activity of the Sun and changes in the Earth's magnetic field. For instance, the radiation dose measured on a satellite in a geostationary orbit (altitude of about 36000 km) was measured to be 50 krad/year by a dosimeter, which was shielded by a 1.89-mm-thick Al sheet [35]. Measurements on the satellite, with the highly elliptical orbit traversing van Allen radiation belts, gave the effective radiation dose of 135 krad/year under 2-mm thick Al shielding [36]. The majority of the Earth observation satellites, including passive atmospheric gas sensors (ENVISAT, OCO-2, GOSAT), are launched in the low Earth close to polar orbits (altitude of 100–1000 km) where the expected radiation dose is much lower, about 2 krad/year for 2-mm-thick Al shielding [37].

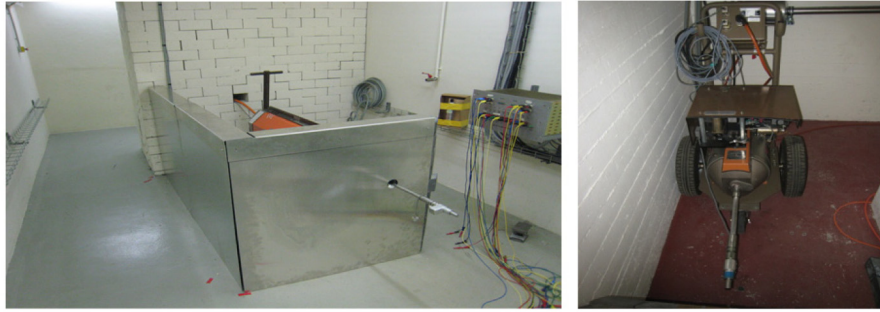


Fig. 1. GMA2500 irradiator with lead/aluminum protection wall (left); GR50 irradiator (right).

Although the components in orbit are primarily exposed to energetic electron and proton radiation, it has been shown that gamma radiation exposure emitted by ^{60}Co sources, with photon energies of 1.17 MeV and 1.33 MeV, produces very similar radiation damage effects at equivalent doses [38]. Therefore gamma rays are suitable and a much lower-cost proxy for evaluating radiation hardness of the components. The irradiation experiments were performed at the MEGA and MILGA facilities at ONERA. The facilities are equipped with commercial ^{60}Co sources GMA2500 (dose rates 3.6 rad/h – 10.8 krad/h) and GR50 (dose rates 0.36 rad/h – 1.8 krad/h) (Fig. 1). Both facilities are panoramic allowing for large volume irradiation (full room volume). Dose cartography of both facilities is calibrated annually utilizing a Radcal active system, and typical transmission and reflection measurements have an error of $\pm 0.01\%$. In order to determine the dosage rate, the distance between the sample and gamma source was varied according to calibration charts. Three dosages were chosen, specifically 10, 30 and 100 krad in accordance to the testing recommendations by the European Space Agency [39]. Moreover, similar doses have been used in the previous experiments reported in the literature [32,33].

Commercial flux-grown KTP and Rb:KTP wafers were cut to the sizes of $12 \times 7 \times 5$ mm along x - y - z crystal axes, respectively. The optical surfaces corresponding to [100] planes were optically polished and left uncoated. One KTP and one Rb:KTP crystal was then periodically poled with the ferroelectric domain periodicity of $38.86 \mu\text{m}$ for type-0 degenerate parametric down-conversion from $1.064 \mu\text{m}$ to $2.128 \mu\text{m}$.

The crystals were irradiated in three steps each time approximately tripling the radiation dose, as recommended by the ESA testing protocol [39]. Following the gamma irradiation of the nonlinear crystals with a predetermined dose, the transmission of each was measured. The transmission was measured using a Lambda 1050 Perkin-Elmer spectrophotometer coupled with an integrating sphere with a diameter of 150 mm. The spectrometer used has a maximum resolution of 0.05 nm in the visible and 0.2 nm in the near-infrared ranges. A Si-photodiode was used in the visible while an InGaAs photodiode in the near infrared. The longest accessible wavelength for this instrument was $1.4 \mu\text{m}$. After the maximum irradiation dose of 100 krad, and transmission characterization, single domain KTP and Rb:KTP crystals were annealed at 150°C for 2 hours. The remaining crystals were kept at room temperature and their transmission characterized again after 24 hours. After the annealing, the transmission of the samples was measured again in the spectral range from visible to mid-infrared. For the transmission measurements in the mid-infrared we employed a FTIR spectrometer (Perkin-Elmer Spotlight 400). In all cases the transmission was measured for the optical beam propagating along the crystal x -axis.

3. Results and discussion

All samples were irradiated in three steps with the calibrated dose rate of 400 rad/hour to reach the dose of 10 krad. The first step lasted 25 hours, following which the samples were removed and their transmission immediately measured. After this, the irradiation continued

for another 50 hours at the same dose rate to reach the cumulative dose of 30 krad. Again the transmission was measured immediately. Then the exposure continued for another 183 hours to reach the final cumulative dose of 100.32 krad. The dose rate is on the high-side of the “low-rate window” recommended for the radiation hardness assurance tests [39]. It is much higher than the dose rates of about 4.8rad/hour and 0.3rad/hour measured on satellites in the geostationary and low-earth orbit, respectively [35,37].

The optical transmission spectra in the visible and near-infrared for the single-domain KTP and Rb:KTP are shown in Fig. 2. The corresponding spectra for the periodically poled crystals PPKTP and PPRKTP are shown in Fig. 3.

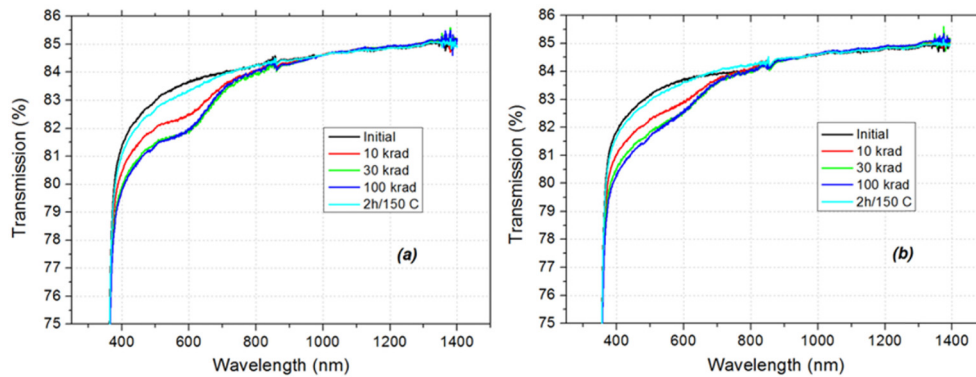


Fig. 2. Measured transmission spectra for KTP (a) and Rb:KTP (b) for varying incident gamma radiation doses.

The black curves in these figures represent the spectra measured before gamma irradiation. The kink seen in the spectra at 860 nm is an artifact related to the change of the detectors/gratings in the spectrophotometer. The strongest decrease in absorption in all samples was in the visible spectral range ranging from 380 nm, i.e. close to the bandgap and down to the wavelength of 800 nm. The largest increase in absorption happened after initial irradiation step by 10 krad. Increasing the dosage we observed that the transmission tended to saturate at dosage of 30 krad. Thus, further increasing the dosage to 100 krad showed a minor effect on the overall transmission. After gamma irradiation single-domain KTP and Rb:KTP crystals were thermally annealed at 150°C for 2 hours and the transmission of each sample was re-measured. Both samples showed improved transmission in the visible range, approaching the measured initial transmission values prior to gamma irradiation.

The transmission spectra before and after gamma irradiation in PPKTP and PPRKTP are shown in Fig. 3 (a) and (b), respectively. The conditions of the irradiation were equivalent to those used in the case of single-domain samples. The qualitative behavior of the irradiated periodically structured crystals is very similar to that observed in the single-domain samples. Namely, the absorption is induced in the same spectral range and it saturates after irradiation with the dose of 30 krad. After reaching the target cumulative dose of 100 krad and transmission characterization the samples were left at room temperature for 24 hours and their transmission was measured again. The results show that the induced absorption does not decrease appreciably, i.e. color center relaxation is very slow at the temperature of 24°C.

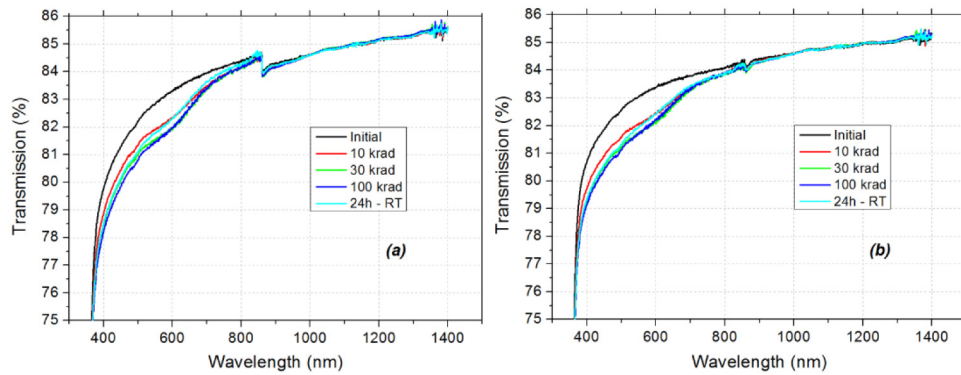


Fig. 3. Measured transmission spectra for PPKTP (a) and PPRKTP (b) for varying incident gamma radiation doses.

For greater clarity, we have summarized the irradiation results for all samples which are shown in Fig. 4(a). We show the measured transmission difference between the initial and 30 krad irradiated samples, since this is where saturation of the transmission was found. For KTP and RKTP we measured a maximum transmission difference approaching 2% and 1.5% respectively at around 600 nm. For PPKTP and PPRKTP, we measure a maximum transmission difference of 1.5%. Although radiation-induced absorption is systematically lower in poled crystals, the difference is too small to warrant strong conclusions.

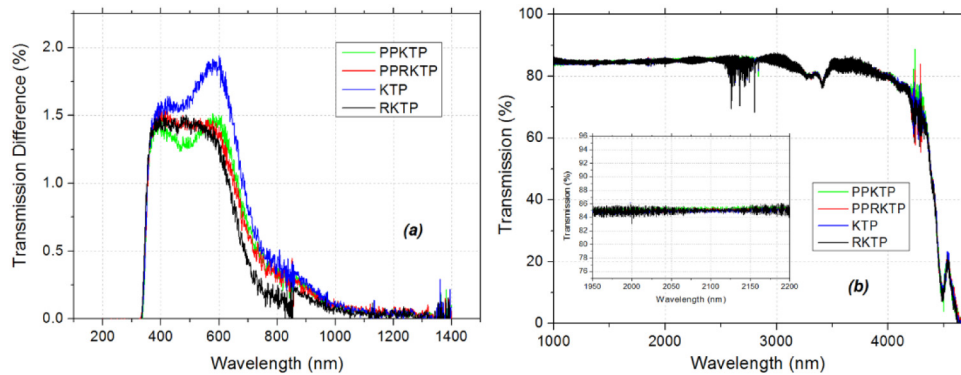


Fig. 4. Measured transmission difference from the initial to 30 krad irradiated samples (a); post irradiation FTIR scan over the infrared range of the samples (b).

The difference might be related to the different concentration of native defects in the crystals. Although single domain and periodically poled samples came initially from the same crystal wafers, for poling we always select parts of the wafers with the lowest ionic conductivity, which directly related to the parts of the wafer with the lowest concentration of potassium and oxygen vacancies. It has been shown that these vacancies play a crucial role in stabilizing color-centers induced in KTP isomorphs by UV light [27].

Finally, the sample transmission at wavelengths longer than 1 μm was measured using a FTIR spectrophotometer. The results are shown in Fig. 4(b). The single domain samples have been annealed at 150°C for 2 hours before this measurement while the PPKTP and PPRKTP were kept at 24°C without annealing step. We paid particular interest to any long term changes around 2 μm , due to the relevance to 1 μm -pumped down-conversion schemes for spaceborne LIDAR instruments. The measurement showed that there is no discernible change in transmission in this spectral region even in the periodically poled samples without high-

temperature annealing. The transmission spectra correspond to those reported in KTP isomorphs without any ionizing irradiation [40].

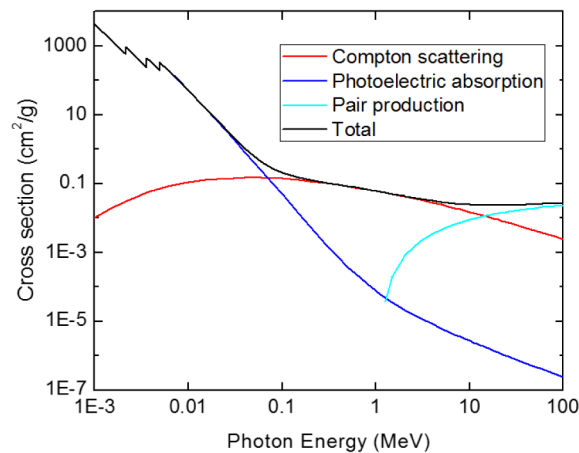


Fig. 5. Interaction cross sections for different processes in KTP as a function of gamma-photon energy.

There are several possible mechanisms by which gamma rays can interact with dielectrics, like KTP isomorphs. To be more specific we used the XCOM program by NIST, to calculate gamma photon interaction cross sections for different processes in KTP [41]. As can be seen from the calculated dependencies in Fig. 5, the main contributing process for the gamma photons emitted by the ^{60}Co source would be Compton scattering with some small contribution from electron-positron pair production. Compton electron energy spans a wide energy spectrum with energies of up to 60% of the gamma quantum for scattering at 180° . From the cross section data in Fig. 5 we can estimate that the Compton electron production rate will be about $4 \times 10^8 \text{ s}^{-1} \text{ cm}^{-3}$ at the incident gamma dose rate of 400 rad/h. Some of those electrons at high energies will leave the crystal; the others will produce secondary electrons which eventually will end up building up a space charge in the crystal volume. It is well-established that Compton scattering of gamma rays can produce a space charge and associated strong internal electric fields in dielectrics [42,43]. The space charge field will relax with a characteristic Maxwell relaxation time, $\tau = \epsilon \epsilon_0 / \sigma$, where ϵ , ϵ_0 , σ are the dielectric constant, the permittivity of free space, and the electrical conductivity of the crystal, respectively. In KTP isomorphs used in this study with the typical ionic conductivity of 10^{-6} S/m and the low-frequency dielectric constant in the range of 10^3 [44], the relaxation time will be in the range of 10 ms. First it should be stressed that the electric field produced by the space charge in our periodically poled samples was not strong enough to modify the QPM structure. This has been verified by not finding any difference in the quasi-phase matched second harmonic generation efficiency before and after radiation exposure with the dose of 100 krad.

The spatial charge relaxes in KTP and RKTP by redistribution of potassium ions K^+ and vacancies, (V_{K}) as well as free charge carriers both, intrinsic and induced by the radiation in the conduction and the valence bands. Part of the secondary electrons will have low enough energy (electron work function in KTP is about 4.5 eV [45]) to be bound in the valence orbitals of the TiO_6 structural groups, which were ionized before by the gamma radiation or the Compton electrons. In KTP the electronic states of these structural groups are mostly contributing to the states at top of the valence band and at the bottom of the conduction band [46]. The electrons with higher energy could be captured with simultaneous generation of electron-hole pairs in the process similar to impact ionization in solids. The fact that the gamma-induced absorption centers can be readily annealed at the temperatures as low as 150°C , as well as similarity of the absorption spectra, indicate that these centers could be of

the same origin as those produced by optical irradiation with intense blue-UV pulses. These centers are related to self-trapped free electrons and holes at the $\text{Ti}^{4+}/\text{Ti}^{3+}$ and O^{2-}/O^- , respectively, with stabilization provided by mobile potassium vacancies [27,47,48].

Comparison of the induced absorption measured in our experiments with the measurements reported in the literature [32–34] indicates that the absolute value of the induced absorption depends much stronger on the gamma radiation dose rate than on the cumulative dose. That would be the case if the processes of free carrier generation, recombination as well as color center self-annealing by the generated phonons are competing. For different radiation dose rates the balance among these processes will be reached at different total radiation doses and at these doses one would expect saturation of the induced absorption.

4. Conclusions

We have investigated optical absorption induced by gamma radiation in KTP, Rb:KTP, PPKTP and PPRKTP nonlinear crystals with the aim of radiation hardness assurance tests for possible application in spaceborne 2 μm LIDAR missions. The cumulative radiation doses up to 100 krad with the dose rate of 400 rad/hour which were employed in this study significantly exceed the levels expected in a low Earth orbit where such instruments will be located. The measurements reveal that the main effect of the gamma radiation at the levels employed here is to induce additional absorption in the visible spectral range, while the changes in optical transmission in the range between 1 μm and 4 μm were not measurable. Moreover, the structure of periodically poled crystals was not impacted by the radiation. Investigation shows that the induced color centers could be readily annealed at temperatures of 150°C and higher, while they remained stable at room temperature. The characteristics of the induced color centers seem to be very similar to those generated by high intensity picosecond optical pulses in blue-ultraviolet spectral region and are attributed to self-trapped excess electrons and holes in the vicinity to $\text{Ti}^{4+}/\text{Ti}^{3+}$ and O^{2-}/O^- centers in the TiO_6 structural groups and possibly self-trapped excitons.

Funding

ESA project GENUIN (No. 4000107439/13/NL/Sfe).